Design of Surface Tailored GNPs Loaded with Doxorubicin Hydrochloride

Hatem A. Sarhan[1], Mohamed A.Amin[2], Wael. A. Hafez[2], Gamal M. S. Zayed2, Montaser M. Shaykoon[3] and Ahmed. M. Abdelsalam[2*]

[1]Department of Pharmaceutics, Faculty of Pharmacy, MiniaUniversity, Minia, Egypt.

[2] Department of Pharmaceutics and Industrial Pharmacy, Faculty of Pharmacy, Al-AzharUniversity, Assuit, Egypt.

[3] Department of Pharmaceutical Chemistry, Faculty of Pharmacy, Al-Azhar University, Assuit, Egypt.

HUMAN JOURNALS

www.ijppr.humanjournals.com

ABSTRACT

Delivering cytotoxic agents to cancer is accompanied with several challenges due to the lack of selectivity and specificity of these agents, where they act against both normal and cancer cell types. However, the ability to target chemotherapeutic agent to cancer without affecting normal cells is promising. On the other hand, the use of Nanoparticulate systems for this purpose could overcome this challenge. Doxorubicin hydrochloride, an anti-cancer agent that is known for its severe side effects mainly cardiomyopathy and renal failure which limits its use. Herein we developed a nanosystem based on gold nanoparticles for the delivery of doxorubicin HCl to cancer. The *in vitro* release behavior of the developed system showed that up to 60% of the loaded doxorubicin HCl was released in acetate buffer pH 5. On the other hand, 10% of the drug was only released in PBS pH 7.4 within 48 hours. Cell viability assay against hepatocellular carcinoma cells (Hep G2 cells) revealed that up to 13.2% of cells were viable at Dox-loaded GNPs concentration of 8 ug/ml, comparatively, 6.1% of cells were viable at the same concentration of free Dox. The developed system was tested against normal cell lines (HL-7702) and found to be less toxic than the free drug. Our developed system seems to be advantageous as cancer drug delivery tool with minimal side effects compared to the parent drug.

1. INTRODUCTION

Nanoparticle-mediated delivery of cancer-fighting agents has shown an enhanced anti-cancer efficacy, while simultaneously reducing the side effects of cancer prevention and treatment [1-3]. Gold nanoparticles (GNPs), also named as gold colloids, have attracted increasing attention due to their ease of synthesis, surface tailoring and unique properties in multidisciplinary research fields. On the other hand, their particular use in drug and gene delivery is one of their most important applications [4-7]. The use of gold nanoparticles in diagnosis and therapy of cancer is one of the most recent studies. It has been shown that they can selectively recognize cancer cells. Their properties render them increasingly attractive candidates for diagnostic and chemotherapeutic substances. Their well-known optical absorption in the visible region (surface Plasmon band, SPB), renders them an ideal nano-objects for medical imaging, drug delivery and even for photo-thermal therapy [8-11]. In order to overcome the severe side effects accompanying cancer therapy, several trials were made to mask the chemotherapeutic agents rendering them harmless to normal cells but active only against cancer cells, several nanoparticulate systems were employed for this purpose, however, GNPs are stated to be useful and safe in this field [12-14]. On the other hand, it was found that PEGylated GNPs are taken by cancer cells more efficiently than non-PEGylated ones. Moreover, the accumulation of naked GNPs is likely to take place in liver and spleen (reticuloendothelial system), PEGylated GNPs lack this type of nanoparticle accumulation making them an excellent sustained drug delivery tools [15, 16]. Doxorubicin hydrochloride, an anthracycline anti-cancer antibiotic was chosen as model drug in present study. Doxorubicin acts by binding to DNA-associated enzymes, intercalate with DNA base pairs, and targeting multiple molecular targets to produce a range of cytotoxic effects that results in cancer cell apoptosis.However, this effect further spread to affect normal cells leading to a series of adverse effects including renal failure, liver toxicity, indirect brain toxicity and most commonly cardiomyopathy[17-19]. In present work, we reported the synthesis of PEGylated GNPs loaded with doxorubicin hydrochloride for an efficient delivery to cancer cells through a pH-sensitive hydrazone linker. Simple chemical modifications were carried out over the commercially available polyethylene glycol making it suitable to self-assemble over the GNPs surface with the simultaneous loading of Dox HCl. It was found that the hydrazone linker is efficiently hydrolyzed in the acidic cancer environment leading to release of Dox HCl. Fortunately, this linker suffers a weak hydrolytic activity in the normal pH values;

Citation: Ahmed. M. Abdelsalam et al. Ijppr.Human, 2016; Vol. 6 (4): 653-670.

654

making it safe towards normal cells, such strategy may reduce the known adverse effects of this drug [13, 20].

2. MATERIALS AND METHODS

2.1 Materials

Hydrogen tetrachloraurate trihydrate (HAuCl$_4$.3H$_2$O) was purchased from Acros organics, Belgium. Tri-sodium citrate dihydrate was supplied by Fisher Scientific Company, USA. Polyethylene glycol 2000 Daltons was purchased from Alfa Aeser, Germany. Doxorubicin hydrochloride was provided by Beijing Mesochem Technology Company, Beijing, China. Para-toluene sulphonyl chloride was purchased from Loba Chemi, Mumbai, India. AIBN (azo-bis-(isobuteronitrile)), hydrazine hydrate and thionyl chloride were purchased from Sigma Aldrich, Germany. Potassium iodide and anhydrous sodium sulphate were supplied from El-Nasr Pharmaceutical Chemical Company, Egypt. Thioacetic acid was purchased from Tokyo Chemical Industries (TCI), Tokyo, Japan. 11-bromoundecene was purchased from Waco Pharmaceutical Company, Japan. Thioglycollic acid was purchased from Acros Organics, Belgium. Dialysis tubing (MWCO 12-14 kd) was provided by Serva Electronics GmbH, Heidelberg, Germany. All the solvents were dried over molecular sieve 4-8 mesh before use.

2.2 Preparation and characterization of Dox-PEG-undecanethiol conjugate

The Dox-PEG-undecanthiol conjugate was chemically synthesized as illustrated in scheme 1.The conjugate was characterized using IR (Nicolet 6700 FT-IR instrument, Thermo-Fischer scientific corporation. Maddison, USA) and NMR spectroscopy (Bruker Avance III 400 MHz for ^{1}H and 100 MHz for ^{13}C (Bruker AG, Switzerland) with BBFO Smart Probe and Bruker 400 AEON Nitrogen-Free Magnet).

2.2.1 Synthesis of α-tosyl-Ɔ-hydroxyl polyethylene glycol (compound 1)

Monotosyl-PEG was synthesized according to literature procedures[21-24]. Briefly 10 g PEG 2kd (5 mM) were dissolved in 500 ml of dry DCM and the resulting clear solution was chilled to 0°C in an ice bath under nitrogen atmosphere, 1.738 g of silver oxide (1.5 equivalents) and 332 mg of potassium iodide (0.4 equivalents) were added to the stirring chilled solution. Para-toluene sulfonyl chloride 1 g (1.05 equivalents) was dissolved in sufficient volume of DCM and quickly added to the rapidly stirring reaction mixture. The

Citation: Ahmed. M. Abdelsalam et al. Ijppr.Human, 2016; Vol. 6 (4): 653-670.

655

reaction was left under nitrogen for 2-4 hrs. Completion of the reaction was monitored by TLC, where fainting of tosyl spot indicated the reaction progression. The reaction mixture was then filtered to remove inorganic salts, washed with water, dried over anhydrous sodium sulfate, concentrated to a small volume by rotary evaporation, precipitated in cold diethyl ether and dried under vacuum. (Yield 8.5 g, 78.9 %).

IR (KBr): 3440 (O-H stretching), 3061 (C-H stretching aromatic), 2884, 2770 (C-H stretching aliphatic), 1641 (C=C stretching alkene), 1467 (C-H bending aliphatic), 1344 (O-H bending), 1114 (C-O-C stretching), 948,842, 555 cm^{-1}.

^{1}H NMR (400 MHz, DMSO) δ ppm: 7.78 (2H, d), 7.48(2H, d), 4.47 (1H, s, OH), 4.14 (2H, t, -CH$_2$CH$_2$-OH), 3.70 (2H, t, CH$_2$CH$_2$OsT) 3.60 (m, PEG backbone) 3.35 (2H, t, CH$_2$CH$_2$OsT), 2.44 (3H, s, CH$_3$).

^{13}C NMR (100 MHz, DMSO) δ ppm: 145.25, 133.23, 130.53, 127.99, 126.02, 72.84, 70.32, 68.43, 60.80, 21.49.

2.2.2 Synthesis of polyethylene glycol ethylthioacetate (compound 2)

Synthesis of polyethylene glycol ethylthioacetate was described in literature [25, 26]. Briefly, in 100 ml rounded bottom flask, 5 gm (2.4 mM) of compound 1 was dissolved in 60 ml dry ethanol under nitrogen atmosphere with gentle heating followed by the addition of 482 mg (5 equivalents) sodium hydroxide. Thioglycollic acid 1.11 g (5 equivalents) was mixed with 10 ml dry ethanol and added to the reaction mixture under nitrogen in a dropwise manner via a syringe and the reaction was refluxed under nitrogen for 48 hours. The mixture was then cooled to room temperature, quenched with dilute hydrochloric acid and solvent was evaporated to dryness under vacuum. The solid residue was re-dissolved in dichloromethane, washed twice with water, dried over anhydrous sodium sulfate, reduced to a small volume by rotary evaporation and precipitated in cold diethyl ether. The solid residue was filtered, washed with ether and dried in a desiccator, (yield 3.9 g, 81%).

IR (KBr): 3420 (O-H stretching; carboxylic), 2888, 2768 (C-H stretching aliphatic), 1718 (C=O stretching; carboxylic acid), 1467 (C-H bending aliphatic), 1360 (O-H bending), 1115 (C-O-C stretching), 950,842, 529 cm^{-1}.

^{1}H NMR (400 MHz, CDCl$_3$) δ ppm: 3.97(1H, s, CH$_2$OH), 3.83 (2H, t, CH$_2$CH$_2$SCH$_2$), 3.74 (2H, t, CH$_2$OH), 3.6 (m, PEG backbone), 3.48 (2H, s, CH$_2$SCH$_2$COOH), 2.91 (2H, t, CH$_2$CH$_2$SCH$_2$).

Citation: Ahmed. M. Abdelsalam et al. Ijppr.Human, 2016; Vol. 6 (4): 653-670.

656

^{13}C NMR (101 MHz, DMSO) δ ppm: δ 170.55, 77.14, 72.84, 70.71, 70.32, 69.69, 68.01, 65.98, 63.51, 60.79, 33.77, 31.62, 15.72, 14.15.

2.2.3   Synthesis of S-(11-bromoundecyl) thioacetate (compound 3)

Compound 3 was synthesized according to the procedures described by *Moldtand coworkers*[27]. In brief, to 500 ml rounded bottom flask 11-bromoundecene (4 gm, 3.77 ml, 17.15 mM) was added under nitrogen atmosphere to 250 ml dry toluene (previously dried and purged with nitrogen for half an hour) followed by the addition of thioacetic acid (7.428 gm, 6.96 ml, 0.097 M, 5.7 mole equivalent), 0.2 M solution of AIBN was added and the reaction was refluxed under nitrogen for three hours. the reaction was cooled down to room temperature and washed several times with saturated sodium bicarbonate solution (3 x 200 ml) where the organic phase was separated and dried over anhydrous magnesium sulfate, toluene was removed by rotary evaporation and the crude product was purified by column chromatography using hexane: methylene chloride 4:1 over silica gel (yield 3.7 g, 69.7 %).

^{1}H NMR (400 MHz, DMSO) δ ppm: 3.47 (2H, t, CH_2CH_2Br), 2.81 (2H, t, $CH_2CH_2SCOCH_3$) 2.30 (3H, s, CH_2SCOCH_3), 1.80 (2H, t, $CH_2CH_2SCOCH_3$), 1.50 (2H, t, CH_2CH_2Br), 1.26 (14H, m, compound backbone).

2.2.4   Synthesis of carboxy-polyethylene glycol undecanethioacetate (compound 4)

Synthesis of compound 4 was based on the Williamson ether synthesis in which an alkoxide is prepared by the interaction of alcohol with an appropriate alkali followed by the addition of the alkyl halide. In brief2 g of compound 2 (0.964 mM) was allowed to melt in 100 ml rounded bottom flask over an oil bath with gentle stirring followed by the addition of 385.6 mg of sodium hydroxide (10 equivalents) and the mixture was left stirring for two hours at 110°C. This was followed by the addition of 1.193 g of compound 3 (4 equivalents) previously dissolved in 50 ml of dry acetonitrile and the reaction was refluxed for 24hours under nitrogen atmosphere. The reaction mixture was then cooled to room temperature and neutralized with dilute hydrochloric acid. The mixture was rotary evaporated to dryness, re-dissolved in dichloromethane, washed with water and dried over anhydrous sodium sulfate. The dry DCM was concentrated to a small volume, precipitated in cold diethyl ether and dried under vacuum (yield 1.4 g. 63%).

Citation: Ahmed. M. Abdelsalam et al. Ijppr.Human, 2016; Vol. 6 (4): 653-670.

657

IR (KBr):3431 (O-H stretching; carboxylic), 2890, 2768 (C-H stretching aliphatic), 1735 (C=O stretching; carboxylic acid), 1664 (C=O stretching; thioester), 1467 (C-H bending aliphatic), 1359 (O-H bending), 1115 (C-O-C stretching), 950,842, 531 cm^{-1}.

^{1}H NMR (400 MHz, CDCl$_3$) δ ppm, 3.81 (2H t, CH$_2$CH$_2$S), 3.64 (m, PEG backbone), 3.45 (2H s, SCH$_2$COOH), 2.85 (2H t, CH$_2$CH$_2$OCH$_2$), 2.67 (2H t, CH$_2$CH$_2$SCOCH$_3$), 2.49 (2H t, CH$_2$CH$_2$SCH$_2$COOH), 2.31 (3H s, CH$_3$COSCH$_2$), 1.66 (2H t, CH$_2$CH$_2$SCOCH$_3$), 1.54 (2H t, CH$_2$CH$_2$OCH$_2$), 1.26 (14H m, alkyl chain).

2.2.5 Synthesis of undecanethiol- polyethylene glycol hydrazide (compound 5)

Synthesis of compound 5 was based on the ordinary acid activation using thionyl chloride. 1 g of compound 4 (0.434 mM) was dissolved in 30 ml dry DCM in 100 ml rounded bottom flask followed by the dropwise addition of 158 ul of thionyl chloride (5 equivalents) in an ice bath. The reaction was left under vigorous stirring for 4 hours at 4°C then for 6 hours at room temperature. DCM and Excess thionyl chloride were removed by distillation and the residue of the acid chloride was redissolved immediately in 20 ml DCM and treated with 66 mg hydrazine monohydrate (3 equivalents) and a drop of triethylamine in an ice-bath and the reaction was left for an extra 6 hours. The mixture was then filtered, evaporated to dryness and the residue was dissolved in DCM and treated with cold diethyl ether to separate the product as brownish to dark yellow precipitate which was filtered and dried in vacuum. (Yield 0.7 g, 70%).

IR (KBr): 3397.2, 3303.5, (N-H stretching, aliphatic primary amine) 3245.58, 3150, 3040 (N-H stretching band, primary amide), 2918, 2701(C-H stretching, aliphatic), 2581 (moderate S-H stretch). 1631.82 (C=O stretching, primary amide), 1576.3 (N-H bending band, primary amide), 1403.57 (C-N stretching, primary amide), 1114 (C-O-C stretching), 610.15 (N-H waging), 576 and 499 cm-1.

^{1}H NMR (400 MHz, DMSO) δ ppm, 8.16 (1H s, CO-NH-NH2), 3.71 (2H s, CO-NH-NH2) 3.68, 3.50 (m, PEG backbone), 3.41 (2H s, S-CH2-CO) 2.90 (2H t, CH$_2$CH$_2$OCH$_2$), 2.78 (2H t, CH$_2$CH$_2$SCOCH$_3$), 2.68 (2H t, CH$_2$CH$_2$SCH$_2$COOH), 1.67(2H t, CH$_2$CH$_2$SCOCH$_3$), 1.59 (2H t, CH$_2$CH$_2$OCH$_2$), 1.23 (14H m, alkyl chain) , 1.09 (1H t, CH2-SH).

Citation: Ahmed. M. Abdelsalam et al. Ijppr.Human, 2016; Vol. 6 (4): 653-670.

658

2.2.6 Synthesis of doxorubicin HCl – polyethylene glycol-undecanethiol conjugate through pH-sensitive hydrazone linkage (compound 6)

Several reported methods described the synthesis of Dox-polymer conjugate through the hydrazone linkage[20, 28, 29]. The reaction was carried out in acidic conditions. Briefly, 162 mg of undecanethiol-PEG-hydrazide (0.0571 mM) were dissolved in 10 ml of dry methanol. In 50 ml rounded bottom flask, under nitrogen atmosphere followed by the addition of 33.11 mg of Dox HCl (0.0571 mM). The mixture was vigorously stirred under nitrogen for 5 minutes before the addition of 120 ul of glacial acetic acid. The reaction was left under nitrogen in the dark for 24 hours at room temperature. The reaction progression was monitored by TLC using methanol: chloroform 4:6. (RF, DOX 0.3, DOX-CONJ 0.7). Methanol was then removed by drying under vacuum, followed by the addition of chloroform to dissolve the PEG-Dox conjugate which was further filtered to remove unreacted DoxHCl. The chloroform solution was then concentrated to a small volume by rotary evaporation, precipitated in cold diethyl ether and dried under vacuum, yield (98.2 mg, 48.6%).

2.3 Preparation and characterization of gold nanoparticles

2.3.1 Preparation of citrate capped GNPs

Gold nanoparticles (GNPs) were prepared according to literature procedures[30-32], in which hydrogen tetrachloroaurate was brought to boiling and reduced by rapid addition of sodium citrate. Briefly, an optimized gold/citrate ratio was prepared as follows, in 100 ml rounded bottom flask. 97 ml of distilled water and 1 ml of 1% $HAuCl_4.3H_2O$ were heated until boiling under reflux, followed by the rapid addition of 2 ml aqueous solution of tri-sodium citrate dehydrate solution. Boiling and stirring were continued for 15 minutes. After that, the heating was ceased and the solution was stirred until it was cooled down to room temperature. Stock solutions of the gold salt (10 mg/ml, 1%) and tri-sodium citrate (100 mg/ml, 10%) were prepared using deionized water and were filtered through 0.22 µm membrane filter.

2.3.2 Preparation of DoxHCl loaded GNPs

Loading of DoxHCl onto GNPs was based on the self-assembly of the Dox-PEG-undecanthiol over the surface of GNPs to obtain GNPs with exposed Dox HCl on their surface (figure 1). Briefly, 5mg of the Dox-PEG-undecanethiol conjugate were added to 25 ml of GNPs colloidal dispersion in order to obtain a final concentration of 200 ug/ml of the

Citation: Ahmed. M. Abdelsalam et al. Ijppr.Human, 2016; Vol. 6 (4): 653-670.

659

Dox-PEG conjugate. The mixture was stirred for 24 hours in the dark, dialyzed against distilled water for 24 hours to remove unbound DOX and polymer and characterized for their size, zeta potential, and morphology.

2.3.3 Characterization of citrate capped and Dox loaded GNPs

2.3.3.1 UV-visible spectroscopy of the prepared nanoparticles

Ultraviolet-visible light absorption spectra of the citrate stabilized and Dox-loaded gold nanoparticles were recorded at room temperature using spectrophotometer (Schimadzu1601-double beam spectrophotometer, Shimadzu Company, Japan).

2.3.3.2 Size and zeta potential measurement of nanoparticles by photon correlation spectroscopy (PCS)

The size distribution and the zeta-potential of the prepared gold nanoparticles before and after drug loading were analyzed by photon correlation spectroscopy PCS using Zetasizer ZSNano (Malvern instruments, UK).

2.3.3.3 Nanoparticles morphological determinations using TEM imaging.

The morphology of the prepared gold nanoparticles was determined by TEM imaging. TEM samples were prepared by dropping gold colloids on carbon-coated copper grids followed by natural drying. The samples were observed on a JEM-100CXII transmission electron microscope (JEOL Ltd, Tokyo, Japan).

2.4 *In-vitro* release behavior of doxorubicin hydrochloride

In order to evaluate the release behavior of doxorubicin HCl from the DOX-PEG-GNPs, 2.5 ml of the DOX-PEG-GNPs were mixed with an equal volume of acetate buffer pH 5 and PBS pH 7.4 to obtain a final PEG-DOX concentration of 0.1 mg/ml, each was sealed in dialysis membrane tubing MWCO 12-14 kd and incubated in 50 ml acetate buffer pH 5 and PBS pH 7.4 respectively. The release was carried out at $37^{o}C$ and 50 rpm in a shaking water bath. Samples were withdrawn from the release medium at predetermined time intervals for 48 hours, the amounts of withdrawn samples were replaced with the same volume of fresh buffer. Released amount of DOX HCl were measured by UV-Vis spectroscopy at 480nm[22, 33-35].

Citation: Ahmed. M. Abdelsalam et al. Ijppr.Human, 2016; Vol. 6 (4): 653-670.

660

2.5 *In-vitro* Cytotoxicity of GNPs-PEG-Dox conjugate against hepatocellular carcinoma (Hep G2) cell line and HL-7702 normal liver cell lines

In order to investigate the cytotoxic activity of GNPs-PEG-Dox against Hep G2 cancer cell lines and HL-7702 normal cells, we prepared 25 ml of citrate-capped GNPs according to the previously described procedures, to which an excess amount (50 mg) of Dox-PEG-undecanethiol was added and left stirring for 24 hours. The prepared volume was centrifuged for 30 minutes at $10x10^3$ rpm (Labnet Microcentrifuge, USA), the supernatant was removed and assayed for unbound drug and polymer conjugate using UV-Vis spectroscopy and the GNPs pellets were redispersed in 1 ml deionized water and filtered through 0.22 um filter. The percentage amount of loaded drug was estimated using the relation:

$$\text{Amount of loaded Dox} = \text{weight of Dox} / \text{weight of Dox- polymer} \times 100$$

The *in vitro* cytotoxicity of the designed GNPs-PEG-Dox was evaluated using the MTT assay, which was performed on HepG2 cancer cell lines and HL-7702 (healthy liver cell lines) (both from Vacsera, Egypt). Both cell lines were maintained in RPMI1640 medium and with 10% (v/v) fetal bovine serum at 37°C in 5% CO_2. Cell lines were seeded into 96-well plates at $1x10^5$ cells/ml. After 24 h, the medium was changed and various concentrations of DOX-loaded gold nanoparticles and free DOX (range from 8, 4, 2to 0.06 ug in culture medium) were added. At intervals of 6 h, the medium was removed and the cells were washed twice with PBS; 25ul MTT dye (5 mg/ml) was added to each well. After 5 h at 37°C, formazan (MTT metabolic product) was resuspended in 200 ul DMSO and the percentage of cell viability was determined by measuring the optical density at 545 nm relative to non-treated cells by a microplate reader[36]. On the other hand, HL-7702 cells were employed to compare anti-cancer effects of free DOX and Dox-loaded gold nanoparticles on healthy cells. The obtained results were subjected to statistical analysis using the Kruskal-Wallis test.

3. RESULTS AND DISCUSSION

3.1 Synthesis and Characterization of Dox-PEG-undecanethiol conjugate

Dox-PEG-undecanethiol was synthesized and characterized as described before. First, the commercially available PEG 2 kd was monotosylated, followed by the conversion of monotosyl-PEG into a monocarboxylic-PEG which was further reacted with bromoundecane thioacetate (protected alkanethiol). The produced mono carboxylic-PEG-undecyl thioacetate

Citation: Ahmed. M. Abdelsalam et al. Ijppr.Human, 2016; Vol. 6 (4): 653-670.

661

derivative was then activated via thionyl chloride and the obtained acid chloride was further reacted with excess hydrazine monohydrate to give the desired hydrazide product. The obtained PEG-hydrazide was then reacted with Dox HCl in 1:1 molar ratio for 24 hours in the presence of glacial acetic acid. The ^{1}HNMR spectrum of the produced PEG-Dox conjugate (figure 2) indicated that the Dox HCl molecule was efficiently bound to the PEG molecule that was indicated by the characteristic Dox HCl peaks.

3.2 Characterization of gold nanoparticles

3.2.1   UV-visible spectroscopy of the prepared GNPs

The synthesized GNPs were characterized for their UV-SPR band and it was found that the produced ruby red color colloidal gold (figure3 a) exhibited a characteristic UV-SPR band at 523 nm (figure3 b). On the other hand the assembled DOX-PEG-UN-SH had no effect on the UV-SPR band of GNPs, instead, the characteristic wavelength maximum of Dox HCl at 480 nm was masked and only the wavelength maxima at 254 nm and 233 nm were noticed (figure 3 c). UV-Vis spectrum for both PEG-conjugated and non-conjugated Dox HCl was also recorded and it was noticed that the maximum wavelength was 480 nm for both materials despite the low concentration of the PEG-conjugated Dox HCl (figure3 d). This observation may be attributed to the co-existence of the characteristic bands of both GNPs and Dox HCl in the same UV region where GNPs band predominates.

3.2.2   Size and zeta potential measurement

The hydrodynamic diameter and zeta potential of both citrate-capped and Dox loaded GNPs were recorded at room temperature (table 1). The obtained results revealed a slight change in the average size from 36 nm (PDI 0.268) to 40 nm (PDI 0.281) before and after drug-polymer loading respectively, which indicated an efficient drug loading[22].On the other hand, the zeta potential changed from -49 mV for citrate-capped GNPs to -20 mV for PEG-Dox loaded GNPs which may be attributed to the positive charge of the incorporated Dox HCl. However, figure 4 illustrates the change in size and zeta potential of both citrate capped and Dox loaded GNPs.

3.2.3   Nanoparticles morphology using TEM imaging

Morphology of the prepared GNPs was estimated using TEM imaging of a freshly prepared colloidal gold dispersion. TEM images showed that the prepared nanoparticles were spherical

Citation: Ahmed. M. Abdelsalam et al. Ijppr.Human, 2016; Vol. 6 (4): 653-670.

662

in shape (figure5). Moreover, it was found that there was no change in the particle shape before and after loading of the drug –polymer conjugate.

3.3 *In-vitro* release behavior of doxorubicin hydrochloride

Doxorubicin hydrochloride release behavior was assessed at different pH values. The UV absorption spectra of DOX at pH 7.4 and 5 were recorded and it was found that changes in pH value had no apparent effect on the UV absorption of DOX (figure 6).

As shown in figure 7 only 10% of the loaded Dox HCl was released in PBS pH 7.4, this type of release is desirable because during circulation in the blood stream where pH is around 7.4, Dox conjugated to nanocarrier would be barely released into the circulation which would reduce the adverse effects that obtained with free doxorubicin HCl. On the other hand at pH 5, up to 60% of the loaded DoxHCl was released within 48 hours in a two stage release manner, namely an initial rapid release stage during the first 10 hours followed by a more sustained release stage. However, this type of pH-dependent doxorubicin release is highly desirable for targeted cancer therapy because it can significantly minimize the amount of free Dox HCl in the bloodstream circulation yet provide a sufficient amount of drug to effectively kill the cancer cells once the nanocarrier reaches cancer tissue.

3.4 *In-vitro* Cytotoxicity of GNPs-PEG-Dox conjugates against hepatocellular carcinoma (Hep G2) cancer cell lines

In vitro cytotoxicity was assessed to evaluate the cytotoxic activity of the designed system in cancerous conditions where the Cell viability using MTT assay revealed that the cytotoxic effect of the designed system was relatively smaller than free doxorubicin as illustrated in figure 8. On the other hand, our developed conjugates still exhibit a prominent inhibition to cancer cells. Moreover, there was no statistical significance between the effects of free and conjugated Dox as shown in table 2. Comparatively, our observation met with some reported results based on polymer-Dox conjugation strategies[29, 35].

On the other hand, the toxic effect of the DOX-loaded GNPs on HL-7702 cells was significantly decreased compared to the toxic effect of free Dox (figure 9).This type of cytotoxicity reduction was of high statistical significance at p< 0.01 as shown in table 2. This result implies that the GNPs-PEG-Dox may have lower side effects on healthy cells. Moreover, the viability of all cells decreased with an increase of DOX in the GNPs-PEG-Dox system.

Citation: Ahmed. M. Abdelsalam et al. Ijppr.Human, 2016; Vol. 6 (4): 653-670.

663

Table 1: Size and zeta-potential measurements of citrated capped and Dox-PEG loaded GNPs

	Hydrodynamic size	Zeta-potential	PDI
Citrate capped GNPs	36 nm	-49 mV	0.268
Dox-PEG-GNPs	40 nm	-20 mV	0.281

Table 2: Non-parametric ANOVA "Kruskal-Wallis test" Showing the p values of the designed system against HepG2 and HL-7702 cell lines

	HepG2 cell line	HL-7702 cell line
p value	0.345	0.001629**

** $p < 0.01$
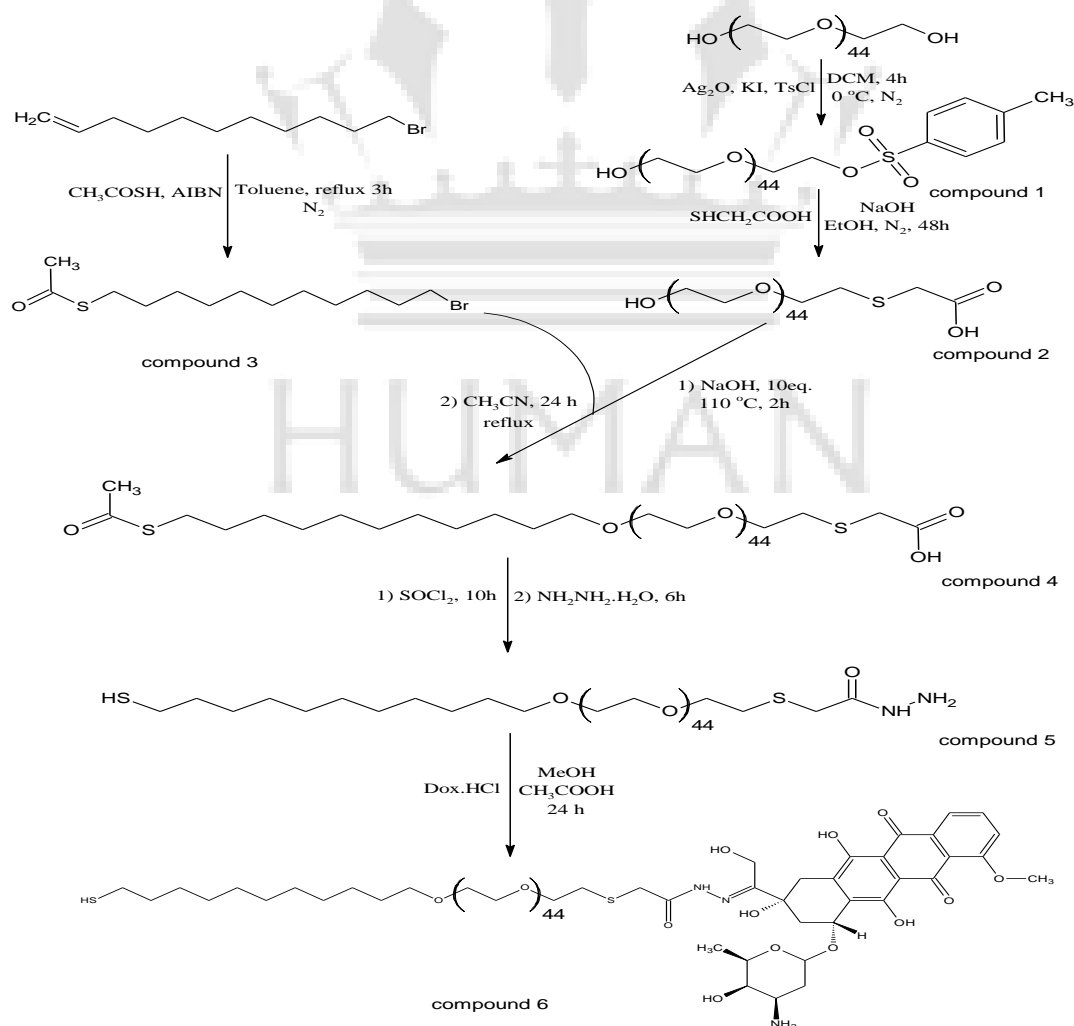
Scheme 1: Synthesis of DOX-PEG-undecanethiol conjugate

Citation: Ahmed. M. Abdelsalam et al. Ijppr.Human, 2016; Vol. 6 (4): 653-670.

664
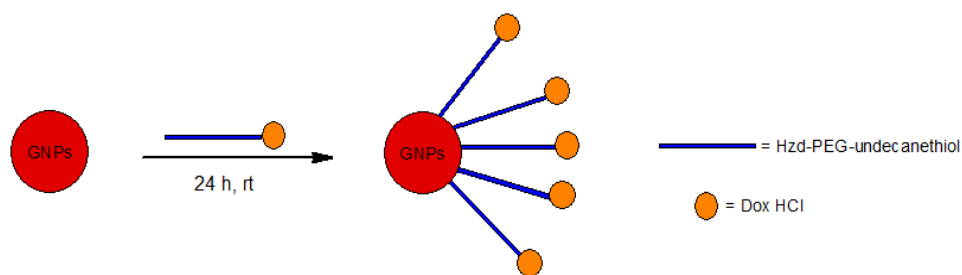
Figure 1: **Self-assembly of Dox-PEG-undecanethiol over the surface of GNPs**
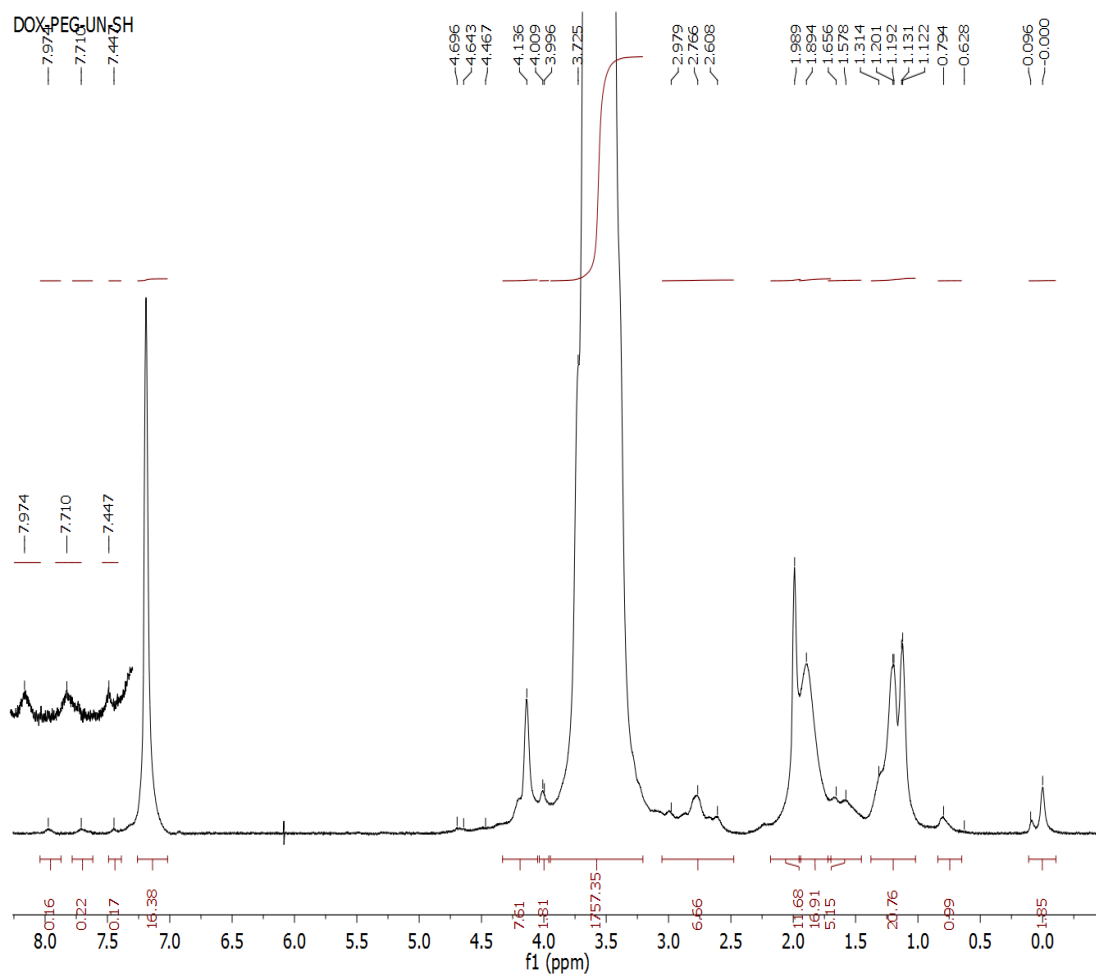
Figure 2: ¹HNMR spectrum of Dox-PEG-undecanethiol conjugate

Citation: Ahmed. M. Abdelsalam et al. Ijppr.Human, 2016; Vol. 6 (4): 653-670.

665

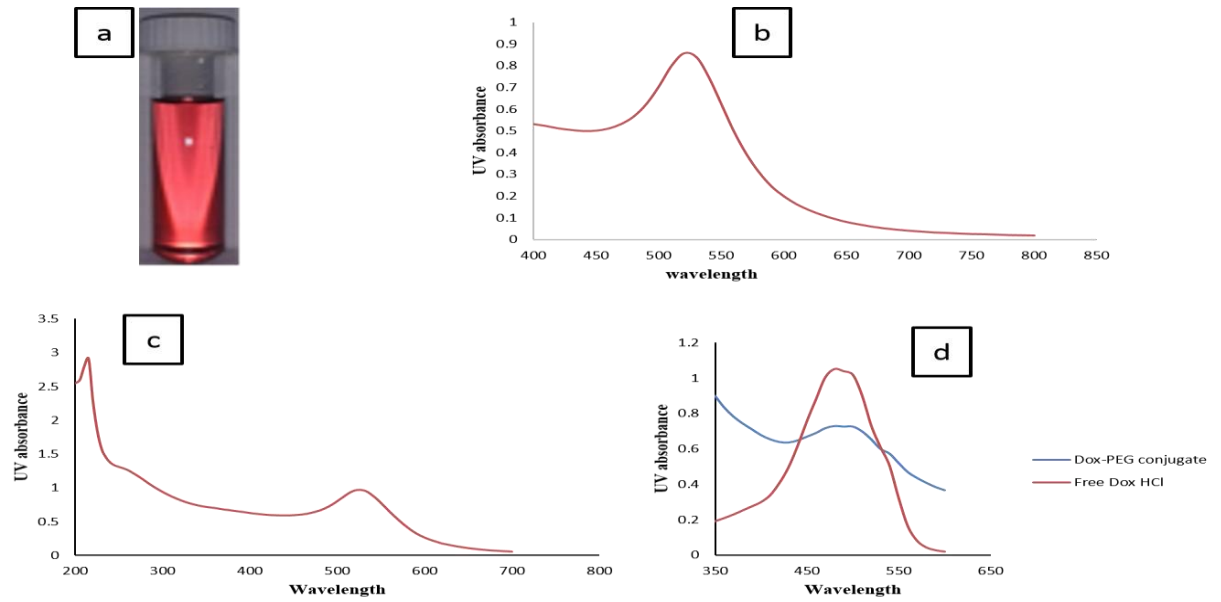**Figure 3: a) Freshly prepared colloidal GNPs, b) UV-SPR of citrate capped GNPs, c) UV-Vis spectrum of GNPs loaded with PEG-Dox conjugate, d) UV-Vis spectrum of free Dox and PEG-Dox**
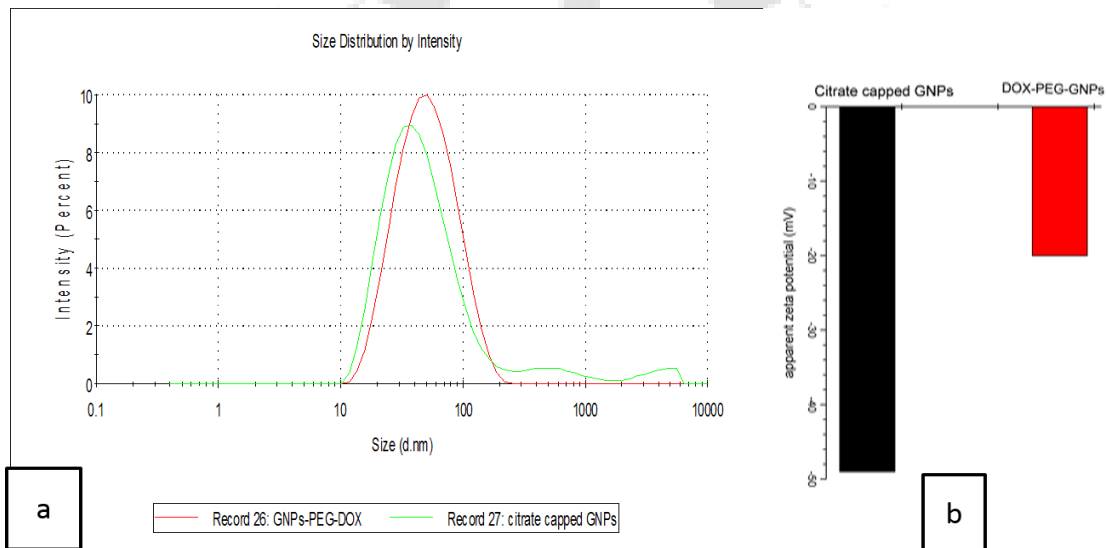

Figure 4: **a) The size distribution of citrate capped GNPs and GNPs-PEG-Dox, b) Apparent zeta-potential of citrate capped GNPs and GNPs-PEG-Dox**

Citation: Ahmed. M. Abdelsalam et al. Ijppr.Human, 2016; Vol. 6 (4): 653-670.
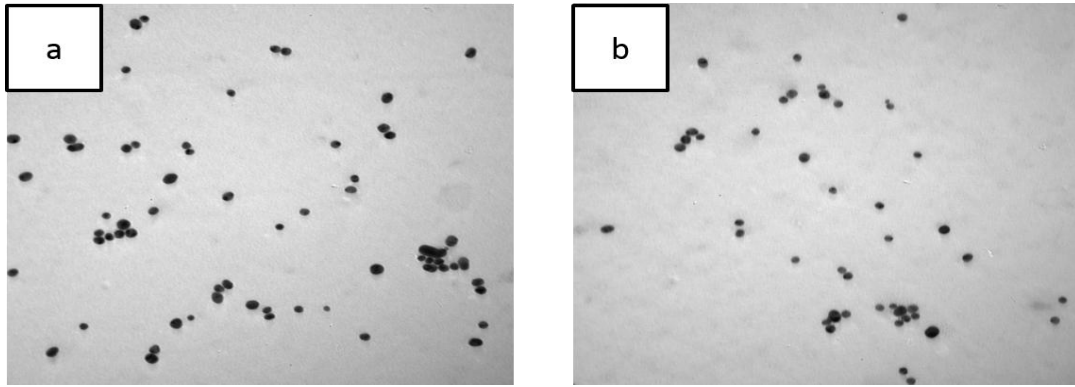
666

Figure 5: TEM images of the prepared GNPs, a) before drug-polymer loading, b) after drug-polymer loading
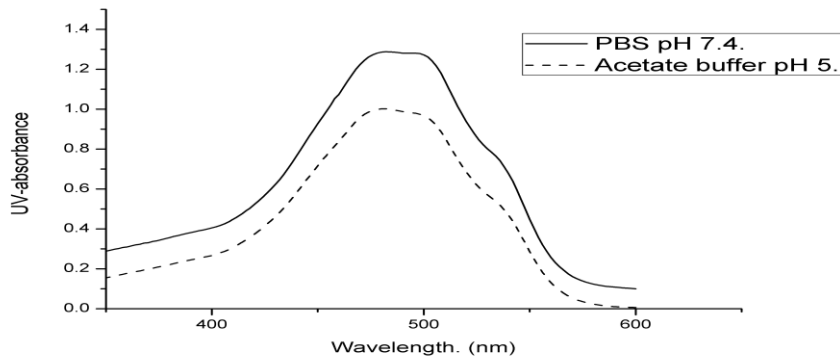

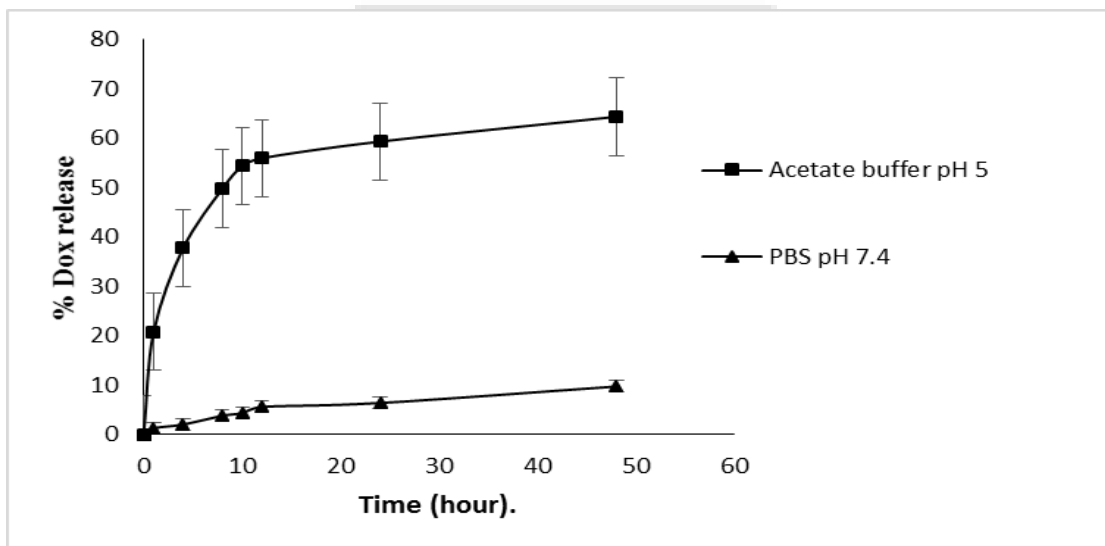**Figure 6: UV-Vis absorption spectra of Dox HCl in PBS pH 7.4 and acetate buffer pH 5**

Figure 7: Doxorubicin release profile in PBS pH 7.4 and acetate buffer pH 5

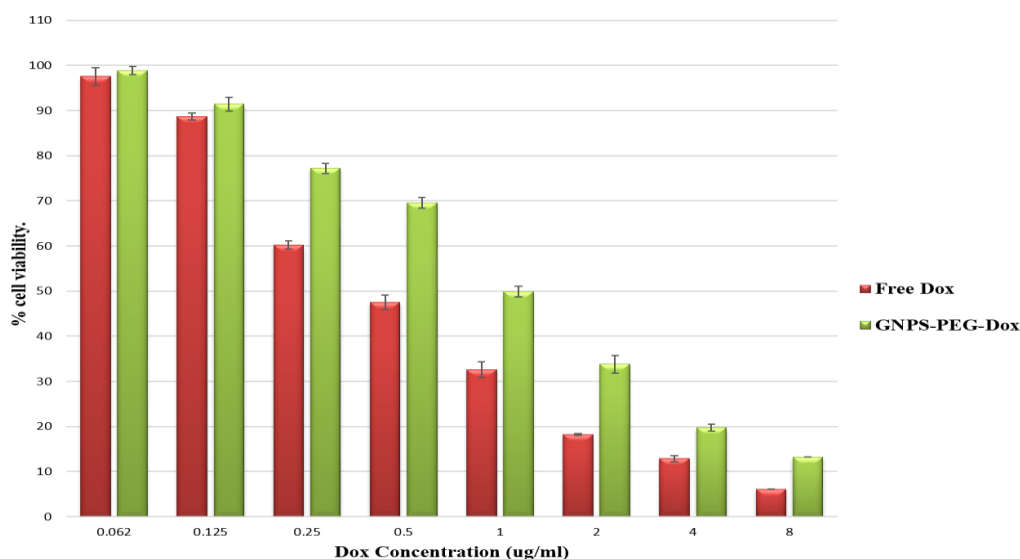*Citation: Ahmed. M. Abdelsalam et al. Ijppr.Human, 2016; Vol. 6 (4): 653-670.*

667

Figure 8: Cell viability (%) of the developed GNPs-PEG-Dox compared with free Dox against Hep G2 cancer cell line (Data are represented as mean ± S.D, Where n=3)
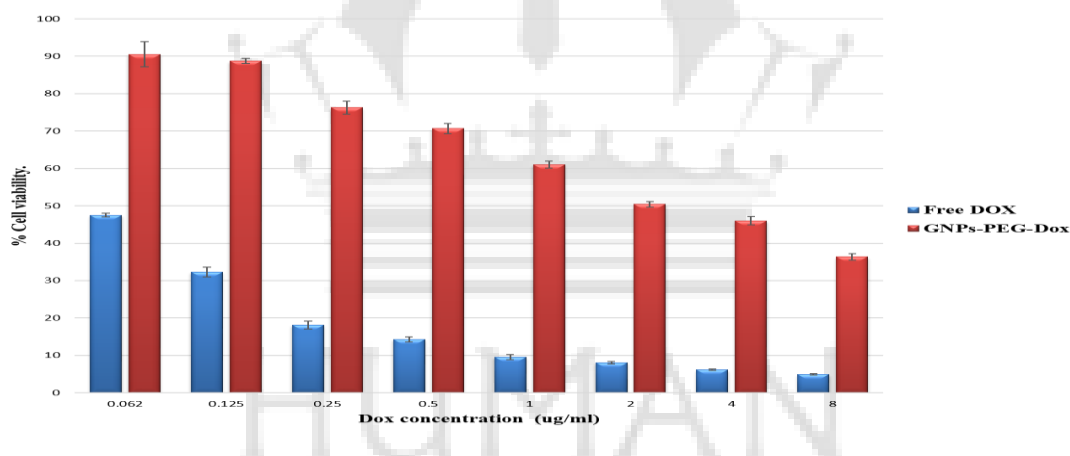

Figure 9: Cell viability (%) of free Dox and GNP-PEG-Dox against HL-7702 normal liver cell lines (Data are represented as mean ± S.D, Where n=3)

4. CONCLUSION

Doxorubicin-PEG conjugate was developed and assembled over GNPs as a nanotherapeutic agent for cancer targeting. The designed system has shown a good *in vitro* cytotoxic activity against the tested cancer cell lines. On the other hand, it has shown higher cell viability in the case of normal cell lines than cancerous cells. This observation proves that our developed nanoconjugate may have significant lower side effects on healthy cells compared to the free

Citation: Ahmed. M. Abdelsalam et al. Ijppr.Human, 2016; Vol. 6 (4): 653-670.

668

drug. It was believed that the designed system would be promising as a passive targeting tool for cancer drug delivery; however, further investigations are under study.

5. REFERENCES

1. Peer D, Karp JM, Hong S, Farokhzad OC, Margalit R, Langer R. Nanocarriers as an emerging platform for cancer therapy. Nat Nano. 2007;2(12):751-60.

2. Petros RA, DeSimone JM. Strategies in the design of nanoparticles for therapeutic applications. Nat Rev Drug Discov. 2010;9(8):615-27.

3. Sun T-M, Wang Y-C, Wang F, Du J-Z, Mao C-Q, Sun C-Y, et al. Cancer stem cell therapy using doxorubicin conjugated to gold nanoparticles via hydrazone bonds. Biomaterials. 2014;35(2):836-45.

4. Li C, Li D, Wan G, Xu J, Hou W. Facile synthesis of concentrated gold nanoparticles with low size-distribution in water: temperature and pH controls. Nanoscale Research Letters. 2011;6(1):1-10.

5. Ghosh P, Han G, De M, Kim CK, Rotello VM. Gold nanoparticles in delivery applications. Advanced Drug Delivery Reviews. 2008;60(11):1307-15.

6. Bhumkar DR, Joshi HM, Sastry M, Pokharkar VB. Chitosan Reduced Gold Nanoparticles as Novel Carriers for Transmucosal Delivery of Insulin. Pharmaceutical Research. 2007;24(8):1415-26.

7. Shaat H, Mostafa A, Moustafa M, Gamal-Eldeen A, Emam A, El-Hussieny E, et al. Modified gold nanoparticles for intracellular delivery of anti-liver cancer siRNA. International Journal of Pharmaceutics. 2016;504(1–2):125-33.

8. Llevot A, Astruc D. Applications of vectorized gold nanoparticles to the diagnosis and therapy of cancer. Chemical Society Reviews. 2012;41(1):242-57.

9. Brigger I, Dubernet C, Couvreur P. Nanoparticles in cancer therapy and diagnosis. Advanced drug delivery reviews. 2002;54(5):631-51.

10. El-Sayed IH, Huang X, El-Sayed MA. Surface plasmon resonance scattering and absorption of anti-EGFR antibody conjugated gold nanoparticles in cancer diagnostics: applications in oral cancer. Nano letters. 2005;5(5):829-34.

11. Kim C-k, Ghosh P, Rotello VM. Multimodal drug delivery using gold nanoparticles. Nanoscale. 2009;1(1):61-7.

12. Connor EE, Mwamuka J, Gole A, Murphy CJ, Wyatt MD. Gold Nanoparticles Are Taken Up by Human Cells but Do Not Cause Acute Cytotoxicity. Small. 2005;1(3):325-7.

13. Ruan S, Yuan M, Zhang L, Hu G, Chen J, Cun X, et al. Tumor microenvironment sensitive doxorubicin delivery and release to glioma using angiopep-2 decorated gold nanoparticles. Biomaterials. 2015;37:425-35.

14. Choi SH, Byeon HJ, Choi JS, Thao L, Kim I, Lee ES, et al. Inhalable self-assembled albumin nanoparticles for treating drug-resistant lung cancer. Journal of Controlled Release. 2015;197:199-207.

15. Liu X, Huang N, Wang H, Li H, Jin Q, Ji J. The effect of ligand composition on the *in vivo* fate of multidentate poly(ethylene glycol) modified gold nanoparticles. Biomaterials. 2013;34(33):8370-81.

16. Bednarski M, Dudek M, Knutelska J, Nowiński L, Sapa J, Zygmunt M, et al. The influence of the route of administration of gold nanoparticles on their tissue distribution and basic biochemical parameters: *In vivo* studies. Pharmacological Reports. 2015;67(3):405-9.

17. Tacar O, Sriamornsak P, Dass CR. Doxorubicin: an update on anticancer molecular action, toxicity and novel drug delivery systems. Journal of Pharmacy and Pharmacology. 2013;65(2):157-70.

18. Singal PK, Iliskovic N. Doxorubicin-Induced Cardiomyopathy. New England Journal of Medicine. 1998;339(13):900-5.

19. Chatterjee K, Zhang J, Honbo N, Karliner JS. Doxorubicin Cardiomyopathy. Cardiology. 2010;115(2):155-62.

20. Wang F, Wang Y-C, Dou S, Xiong M-H, Sun T-M, Wang J. Doxorubicin-Tethered Responsive Gold Nanoparticles Facilitate Intracellular Drug Delivery for Overcoming Multidrug Resistance in Cancer Cells. ACS Nano. 2011;5(5):3679-92.

Citation: Ahmed. M. Abdelsalam et al. Ijppr.Human, 2016; Vol. 6 (4): 653-670.

669

21. Shenoy D, Fu W, Li J, Crasto C, Jones G, DiMarzio C, et al. Surface functionalization of gold nanoparticles using hetero-bifunctional poly (ethylene glycol) spacer for intracellular tracking and delivery. International journal of nanomedicine. 2006;1(1):51.

22. Madhusudhan A, Reddy GB, Venkatesham M, Veerabhadram G, Kumar DA, Natarajan S, et al. Efficient pH dependent drug delivery to target cancer cells by gold nanoparticles capped with carboxymethyl chitosan. Int J Mol Sci. 2014;15(5):8216-34.

23. Woghiren C, Sharma B, Stein S. Protected thiol-polyethylene glycol: a new activated polymer for reversible protein modification. Bioconjugate chemistry. 1993;4(5):314-8.

24. Bouzide A, Sauvé G. Silver(I) Oxide Mediated Highly Selective Monotosylation of Symmetrical Diols. Application to the Synthesis of Polysubstituted Cyclic Ethers. Organic Letters. 2002;4(14):2329-32.

25. Volcker N, Klee D, Hanna M, Hocker H, Bou JJ, Ilarduya Ad, et al. Synthesis of heterotelechelic poly (ethylene glycol) s and their characterization by MALDI-TOF-MS. Macromolecular Chemistry and Physics. 1999;200(6):1363-73.

26. Bogdanov AA. Graft-copolymer stabilized metal nanoparticles. US patent; 2015.

27. Moldt T, Brete D, Przyrembel D, Das S, Goldman JR, Kundu PK, et al. Tailoring the Properties of Surface-Immobilized Azobenzenes by Monolayer Dilution and Surface Curvature. Langmuir. 2015;31(3):1048-57.

28. Etrych T, Mrkvan T, Chytil P, Koňák Č, Říhová B, Ulbrich K. N-(2-hydroxypropyl)methacrylamide-based polymer conjugates with pH-controlled activation of doxorubicin. I. New synthesis, physicochemical characterization and preliminary biological evaluation. Journal of Applied Polymer Science. 2008;109(5):3050-61.

29. Etrych T, Šubr V, Laga R, Říhová B, Ulbrich K. Polymer conjugates of doxorubicin bound through an amide and hydrazone bond: Impact of the carrier structure onto synergistic action in the treatment of solid tumours. European Journal of Pharmaceutical Sciences. 2014;58:1-12.

30. Kumar S, Gandhi KS, Kumar R. Modeling of Formation of Gold Nanoparticles by Citrate Method. Industrial & Engineering Chemistry Research. 2007;46(10):3128-36.

31. Frens G. Controlled nucleation for the regulation of the particle size in monodisperse gold suspensions. Nature. 1973;241(105):20-2.

32. Turkevich J, Stevenson PC, Hillier J. A study of the nucleation and growth processes in the synthesis of colloidal gold. Discussions of the Faraday Society. 1951;11(0):55-75.

33. Che E, Wan L, Zhang Y, Zhao Q, Han X, Li J, et al. Development of phosphonate-terminated magnetic mesoporous silica nanoparticles for pH-controlled release of doxorubicin and improved tumor accumulation. Asian Journal of Pharmaceutical Sciences. 2014;9(6):317-23.

34. del Rosario LS, Demirdirek B, Harmon A, Orban D, Uhrich KE. Micellar Nanocarriers Assembled from Doxorubicin-Conjugated Amphiphilic Macromolecules (DOX–AM). Macromolecular Bioscience. 2010;10(4):415-23.

35. Zhang Y, Yang C, Wang W, Liu J, Liu Q, Huang F, et al. Co-delivery of doxorubicin and curcumin by pH-sensitive prodrug nanoparticle for combination therapy of cancer. Scientific Reports. 2016;6:21225.

36. Asadishad B, Vossoughi M, Alamzadeh I. *In vitro* release behavior and cytotoxicity of doxorubicin-loaded gold nanoparticles in cancerous cells. Biotechnology Letters. 2010;32(5):649-54.

Citation: Ahmed. M. Abdelsalam et al. Ijppr.Human, 2016; Vol. 6 (4): 653-670.

670